

PAPER • OPEN ACCESS

Various Solvents' Effect on the Performance of P3HT:ZnONPs:PC70BM Solar Cell

To cite this article: Abdullah. A. Hussein *et al* 2025 *IOP Conf. Ser.: Earth Environ. Sci.* **1440** 012006

View the [article online](#) for updates and enhancements.

You may also like

- [Ameliorated *in vitro* anti-cancer efficacy of methotrexate loaded zinc oxide nanoparticles in breast cancer cell lines MCF-7 & MDA-MB-231 and its acute toxicity study](#)
Mitesh Joshi and Purvi Bhatt
- [Synthesis, characterization, antimicrobial and electrochemical activities of zinc oxide nanoparticles obtained from sarcopoterium spinosum \(L.\) spach leaf extract](#)
Oskay Kahraman, Riza Binzet, Ersan Turunc et al.
- [Antibacterial effects of *in situ* zinc oxide nanoparticles generated inside the poly \(acrylamide-co-hydroxyethylmethacrylate\) nanocomposite](#)
J Y Del C Pereyra, C A Barbero, D F Acevedo et al.

UNITED THROUGH SCIENCE & TECHNOLOGY

 **The Electrochemical Society**
Advancing solid state & electrochemical science & technology

**248th
ECS Meeting**
Chicago, IL
October 12-16, 2025
Hilton Chicago

**Science +
Technology +
YOU!**

**SUBMIT
ABSTRACTS by
March 28, 2025**

SUBMIT NOW

Various Solvents' Effect on the Performance of P3HT:ZnONPs:PC70BM Solar Cell

Abdullah. A. Hussein^{1*}, Naeemah A. Ibrahim², Tahssen A. Saki³

¹Polymer Research Centre, University of Basrah, Basrah, Iraq

²Southern technical university, Basrah, Iraq

³Department of Chemistry, College of Science, University of Basrah, Iraq

*E-mail: abdullah.hussein@uobasrah.edu.iq

Abstract. Hybrid organic-inorganic solar cells of bulk heterojunction (BHJ) have garnered extensive focus as alternate to all-organic photovoltaics due to their remarkable benefits in integrating organic materials' solution-processability and flexibility with the environmental stability of inorganic semiconductors and high charge mobility. This study describes the development of efficient and air-stable hybrid organic-inorganic BHJ solar cells with broad-spectrum sensitivity supported by mixtures of phenyl-C₇₁-butyric acid methyl ester (PC₇₀BM) and poly 3-hexylthiophene with zinc oxide (P3HT: ZnONPs). The solvents (chlorobenzene, chlorobenzene, and chloroform and mixed CF/CB, CF/DCB) used to deposit the hybrid P3HT: ZnONPs BHJ active layer has a significant effect on the film shape and, therefore, on the photovoltaic performance of the solar cells generated as a result. The characterization techniques used for the film morphology, including X-ray diffraction (XRD) patterns, atomic force microscope (AFM) imaging, and external quantum efficiency (EQE) studies on the devices. It is interesting to note that the efficiency of the devices significantly improves when a specific solvent combination of (CB:CF) is utilized. This suggests the importance of solvent selection in optimizing the performance of the devices. The best property was obtained in the active layer by using chlorobenzene (CB) for the P3HT and dichlorobenzene (DCB) for the PCBM. The improvement in the efficiency with regard to a device with CB:CF was more considerable compared to CF, CB and CB: DCB. With different solvent, a solar cell upon (CB:CF) provides PCE (i.e., Power Conversion Efficiency) of 4.1%, dissimilar to 3.92% for (CB: DCB), 3.9% for (CB) and 3.6% for (CB) devices.

Keyword: Organic-Inorganic, P3HT, ZnONPs, PC₇₀BM, Solar Cell

1. Introduction

The conversion of solar energy to electricity becomes increasingly critical in light of the current energy crisis. Numerous natural resources can be used to generate energy. The conversion of solar energy to electrical energy is called one example of natural resource utilization. For the most part, inorganic solar cells have been the most widely used in the past couple of decades in this direction. However, the disadvantages of these materials, for instance, high production costs and complex fabrication procedures, prompted researchers to investigate low-cost polymer materials and easily processable materials and low-cost polymer materials. For almost a decade, polymer photovoltaics have been the subject of extensive research.



Nevertheless, their commercial properties are limited by their lower power conversion efficiency (PCE)[1, 3]. These drawbacks have been solved by introducing the hybrid (BHJ) idea, regarding the PCE of polymer solar cells has approached 5 percent [4]. However, these values are insufficient to meet actual commercialization standards.

The creation of the hybrid BHJ phase enables bulk separation of photo-induced excitons, while high-mobility electrons are eliminated via the nanophase. Historically, P3HT has been the most frequently utilized p-type material [3, 4] in polymer photovoltaics, accompanied by ZnO NPs as an electron acceptor. Subsequently, in regioregular P3HT, the hole is typically the highly mobile carrier [5], by introducing an electron acceptor, the electron mobility was increased. Conversely, these systems' difficulties arise once morphological modifications affect the P3HT phase as a result of the nanophase introduction[6]. Numerous investigations have been conducted to determine the effect of processing parameters on the blended photoactive nanophase[7].

Additionally, regioregularity and the molecular weight [8] of P3HT have a detrimental effect on the performance of devices composed of P3HT: ZnO NPs. The diode's photovoltage and photocurrent under a specific illumination intensity determine electricity generated by a photovoltaic device[8]. A reasonable strategy is to maximize photocurrent to increase the solar device's PCE. The built-in potential of the solar cell is the difference between the electron donor and acceptor materials' highest occupied lowest unoccupied molecular orbitals, respectively[9]. We evaluate various device geometries and interface topologies to trap more light and efficiently dissociate excitons and transport charges with fewer barriers to photocurrent extraction [10]. Indeed, the solvents utilized to prepare the active layer have substantially impacted its morphology, influencing the photocurrent generation in the devices as previous research [11].

2. Experiment

2.1 Fabrication of Solar Cells Devices

Example Pre-patterned glass slides coated with indium tin oxide (ITO) have an 80 nm thickness and a resistivity of $10\Omega/\text{sq}$ sheet. The ITO substrates used in this study were cleaned ultrasonically using acetone and isopropyl alcohol for ten minutes, then dried at $120\text{ }^\circ\text{C}$ for 10 minutes with ozone-ultraviolet cleaner. To generate the hole-transport layer (HTL), spin-casting was used to create a poly (ethylene dioxythiophene) film PEDOT:PSS solution at a speed of 2000 revolutions per minute for 40 minutes at the top of the ITO substrates and dried for 15 minutes at $140\text{ }^\circ\text{C}$. Next, 10 mg mL^{-1} of P3HT and 10 mg mL^{-1} of PC₇₀BM with and ZnO-NPs mixes in variant solvents (CB), (DCB), (CF), and (CB: CF) were spin-cast in a nitrogen-filled glove box. Then, the active layer was spin-coated at 800 rpm onto the PEDOT: PSS film. The active layer has a 150 nm thickness, while the PEDOT: PSS layer has a 40 nm thickness. Lastly, a thermally evaporated bilayer cathode composed of Al (100 nm) was applied to the polymer layer at a rate of 0.2 nm/s while operating at a high vacuum of $2\times 10^{-5}\text{ Pa}$ to design a device with a 9 mm^2 active area a shadow mask of 1 cm^2 is applied to the active layer.

2.2 Characterization of the Device

Placeholder Current density-voltage (J-V) features of the device were determined using Keithley 2400 Digital Source Meter (a computer-programmed), and photocurrent was produced under irradiation with 100 mW cm^{-2} AM 1.5 G. Spin coating was used to create P3HT: ZnO NPs films. P3HT: ZnO NPs solution for atomic force microscopy (AFM) and UV-vis absorption spectroscopy on glass substrates. The ultraviolet-visible absorption spectra of polymer films

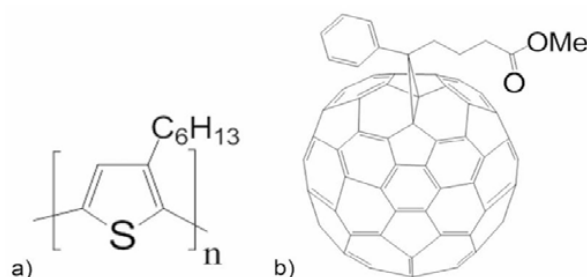


Figure 1. Chemical structures of (a) P3HT and (b) PC₇₀BM.

were acquired using a Varian Cary 5000UV-VIS-NIR spectrometer and a Horiba Jobin Yvon HR800 micro-Raman spectrometer. The solar simulator's generated light intensity was calibrated using a typical solar cell as a reference. The AFM images of the polymer films were acquired in the tapping mode using an AFM (a BRUKER NanoScope IV Multi-Mode Adapter AFM). The film thickness was evaluated using a TencorP-10 Alpha-Step profiler.

The following is a definition of the PCE:

$$\eta = (J_{SC} \times V_{OC}) FF / P_{light},$$

$$FF = (V_{max} \times I_{max}) / (V_{OC} \times I_{SC}),$$

where P_{light} is the incident light's power. For Fe₂O₃NPs, the PCEs of hybrid and new OSCs were calculated [11].

3. Results and discussion

The ultraviolet-visible absorption spectrum of P3HT: ZnO NPs film is seen in Figure (2). (all films have a thickness of 160 nm). BHJ is produced using a variety of solvents, including co-solvents CB, DCB, CF, and CB: CF. A remarkable outcome was found. In comparison to other samples, the P3HT: ZnO NPs BHJ generated with the co-solvent of CB: CF displayed the maximum absorption intensity, with a shift in the visible wavelength range of 400 to 650 nm. The effect of the solvent species on the absorption intensity of the BHJ is seen, demonstrating that the BHJ dissolved in the CB: CF co-solvent absorbs a considerable quantity of photons. The high absorption intensity of light is predicted to improve and rise in the rate of excitons production. This finding may also be explained by a change in the polymer structure's stacking confirmation from high to low crystallinity, in addition to a decrease in intraplate and interplane stacking, which results in poor π - π^* transitions and decreased absorbance [12]. For all solvents, The region of the spectrum below 400nm is occupied by the absorption of ZnO nanoparticles[13]. The XRD results of P3HT: ZnO NPs generated via spin coating with a variety of solvents (CB, DCB, CF, and CB: CF) thermally annealed for 15 minutes at 125°C followed by spin coating are shown in Figure (3). For all solvents, XRD intensity values were recorded for peaks at $2\theta \approx 5.4^\circ$, where the JCPDS 44-0558 determined the reflection of the d100-spacing plane [14]. These numbers represent P3HT's inter-chain spacing related to the interdigitated alkyl chains and serve as an indicator of P3HT's crystallinity [15]. DCB which has bp = 178 °C and CB has bp = 132°C are both high boiling point (bp) solvents, rather than the low-bp solvent, CF which has bp = 61°C were used for BHJ, the intensified intensity was detected at $2\theta \approx 5.4^\circ$ peak.

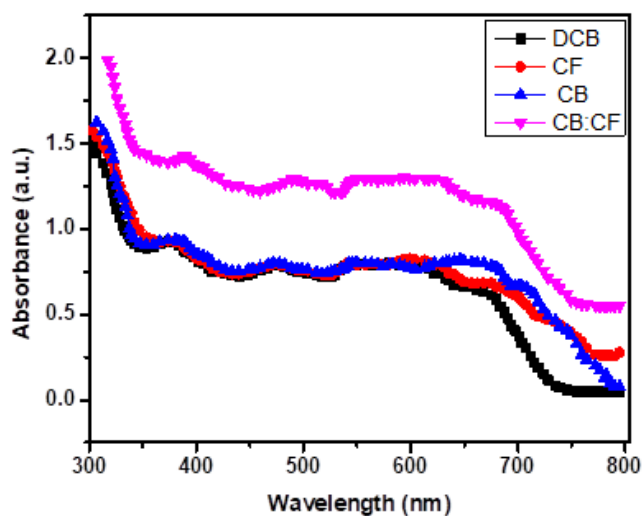


Figure 2. Spectra of UV-vis absorption of films of P3HT: ZnONPs in various solvents CF, CB, DCB, and CB: CF.

The study implies that the BHJ formed from CB and DCB has a more orderly structure and superior crystallinity to CF. In the BHJ, P3HT may take longer to solidify in higher boiling point solvents because of the solvents' slow evaporation rates and the development rate of the slow film may contribute to the formation of a structure that is highly self-organized [16]. During spin casting, P3HT has a competitive film development rate when dissolved in solvents with two distinct vapor pressures and solubilities. The crystallinity of P3HT in BHJ produced from a CF: CB mixture, is higher than that of a mono solvent like CF and CB.

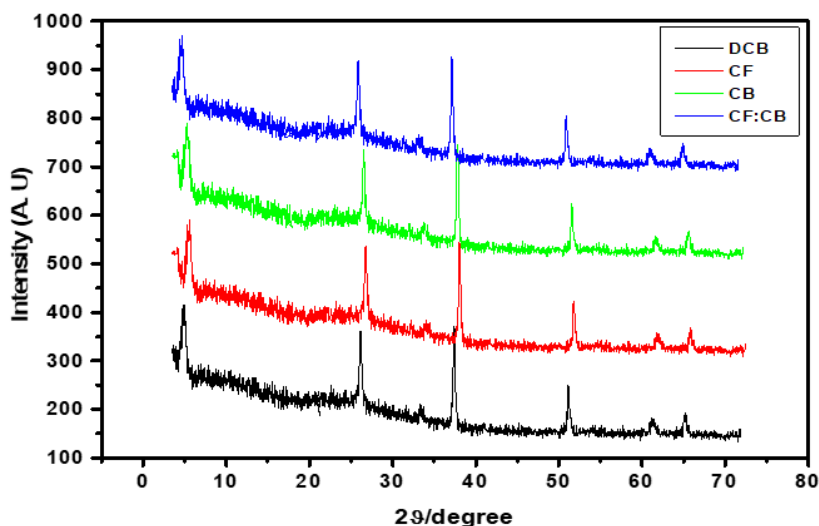


Figure 3: The XRD results of P3HT: ZnONPs films in various solvents DCB, CF, CB, and CF: CB.

Nevertheless, when the BHJ was made from a mixture of CF and DCB, the crystallinity of P3HT was not increased because the vapor pressures of DCB and CF are too dissimilar to allow for a rate of growth that is competitive. Furthermore, following thermal annealing, the crystallinity was enhanced in the BHJ produced from solvents with a low boiling point, especially CF, it possesses a rapid solvent evaporation rate and a high rate of film growth during spin coating [16]. The Raman spectroscopy of PEDOT: PSS/P3HT: ZnONPs film coated on an Al substrate with a variety of solvents such as CB, DCB, CF, and CB:CF co-solvents, is presented in Figure (4). Raman spectroscopy in the 200-2000 cm^{-1} range was used to identify it. Additionally, thermal annealing increased the crystallinity of BHJ produced with solvents with a low boiling point, particularly CF. It has a high solvent evaporation rate and a rapid rate of film growth during spin coating.

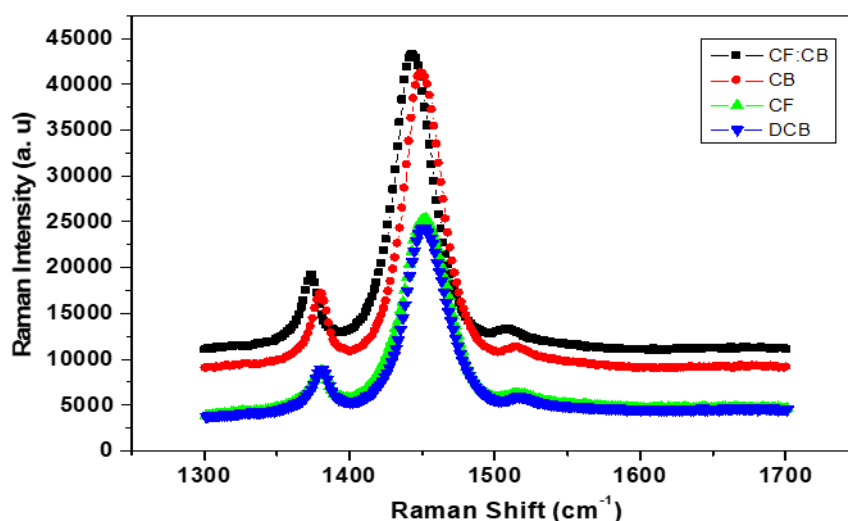


Figure 4: Raman spectroscopy of films containing P3HT:ZnONPs in various solvents (DCB), (CF), (CB), and (CF: CB).

The Raman spectroscopy of PEDOT:PSS /P3HT: ZnONPs films with various solvents (DCB), (CF), (CB), and (CB: CF) is identical to that of P3HT: ZnONPs films due to the absence of Raman features associated with the PEDOT:PSS film and the lack of impact of certain solvents on the PEDOT:PSS/P3HT:ZnONPs films. As a result, the primary in-plane ring skeleton modes exhibit similarity behavior in earlier P3HT, P3HT/ZnONPs, and P3HT:ZnONPs films, as follows: between 1452 and 1468 cm^{-1} (symmetric C=C stretching mode) and 1381-1391 cm^{-1} (C-C intra-ring stretching mode), the inter-ring C-C stretching mode between 1200 and 1210 cm^{-1} , the C-H mode of bending combined with the C-C inter-ring stretch mode between 1180 and 1200 cm^{-1} , and the C-S-C mode of deformation between 720 and 740 cm^{-1} . Similar findings were obtained using pure P3HT in the presence of CB solvent only. [17].

The AFM technique was anticipated to investigate the microstructure of the PEDOT: PSS/P3HT: ZnONPs blends utilizing (DCB), (CF), (CB), and (CB:CF) as solvents. The surface morphologies of the P3HT: ZnO NPsBHJ prepared in various solvents are shown in Figure (5). The root-mean-square (RMS) values for the BHJ dissolved in several solvents were 3.89, 4.13, 3.62, and 6.63nm for DCB, CF CB, solvents, and CB: CF co-solvents, respectively.

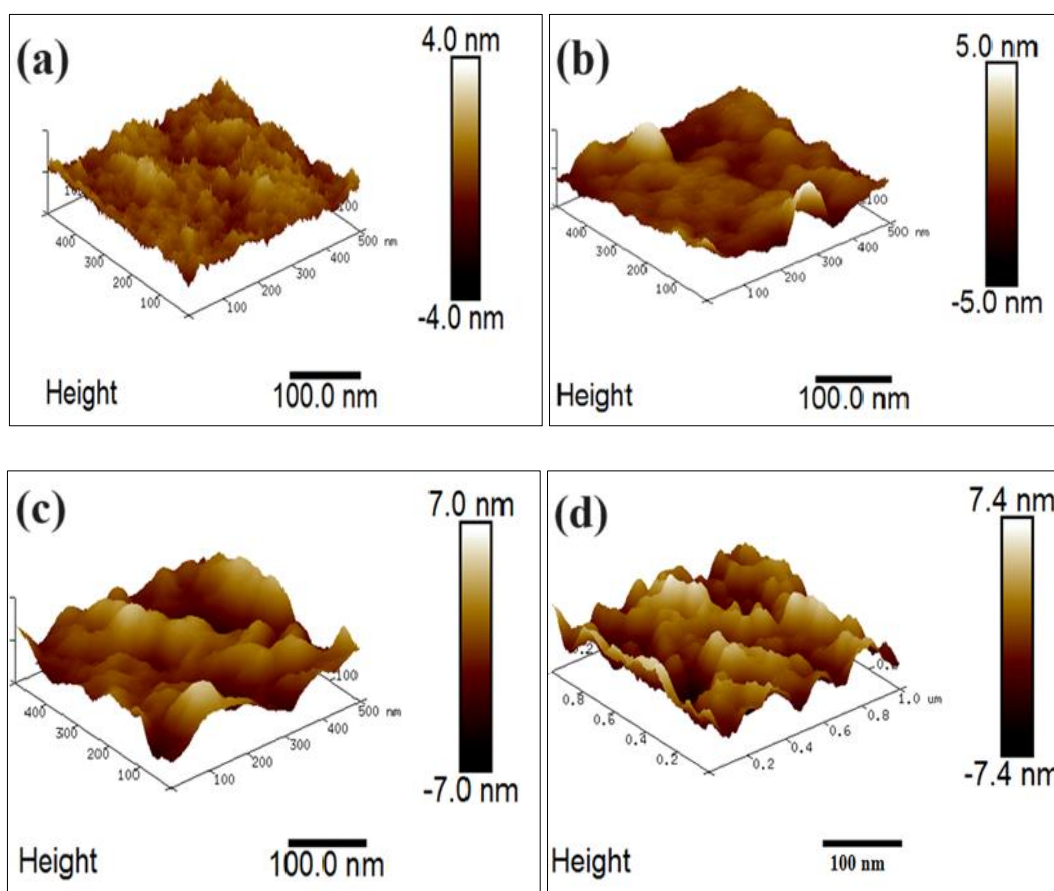


Figure 5: AFM images of P3HT:ZnO NPs films using several solvents (a)DCB, (b)CF, (c) CB, and (d) CB: CF.

The results show that the P3HT:ZnO NPs BHJ generated using the CB:CF co-solvent exhibits a coarser film surface morphology than the samples, as evidenced by the more considerable R_{\max} value of 6.63 nm. These rough film surfaces are resulting in a greater surface area, increasing charge generation efficiency due to the photons' effective incidence. The rough film surface arises from the self-organization of polymers, which enhances forming of ordered structures in a thin layer. This structured arrangement lowers the device's internal series resistance, enhancing the photocurrent [18]. It is worth noting that evaporation rates and solvent solubility might change the surface morphologies of the polymer BHJ. Combining the two solvents alters the co-evaporation solvent's rate, consequently diverse surface morphologies. Additionally, the solvating activation energy considerably affects the film shape, as a suitable solvent may result in a more extended in a solid-state thin film, there is a polymer chain. Once the various solvents alert the surface morphologies, a low solubility, a high vapor density, and a low evaporation rate all point to the CB:CF co-solvent as shown in Table (1). When spin-coated on PEDOT, they provide a rough film surface: PSS:PEDOT/P3HT:ZnO NPs film and a post-annealing temperature of 125 °C.

P3HT:ZnONPs BHJ EQE values were produced in a variety of solvents, including DCB, CF, CB, and CB:CF co-solvents are shown in Figure(5). The P3HT: ZnONPs BHJ produced with the CB:CF co-solvent demonstrated the best peak external quantum efficiency wavelength range of 300–765 nm. We hypothesize that the external quantum efficiency values are correlated to the absorption data, demonstrating that the CB:CF blend layer absorbs considerably more than the other solvents [19].

Table 1. Replace Table 1: The AFM values for P3HT: ZnO NPs BHJ films in various solvents DCB, CF, CB, and CB:CF.

Solvent	R.M.S $\times 10^{-9}$ (m)	R _a $\times 10^{-9}$ (m)	R _{max} $\times 10^{-9}$ (m)
DCB	4.32	4.11	36.3
CF	4.44	4.13	40.4
CB	6.44	6.21	55.8
CB:CF	6.94	6.65	64.2

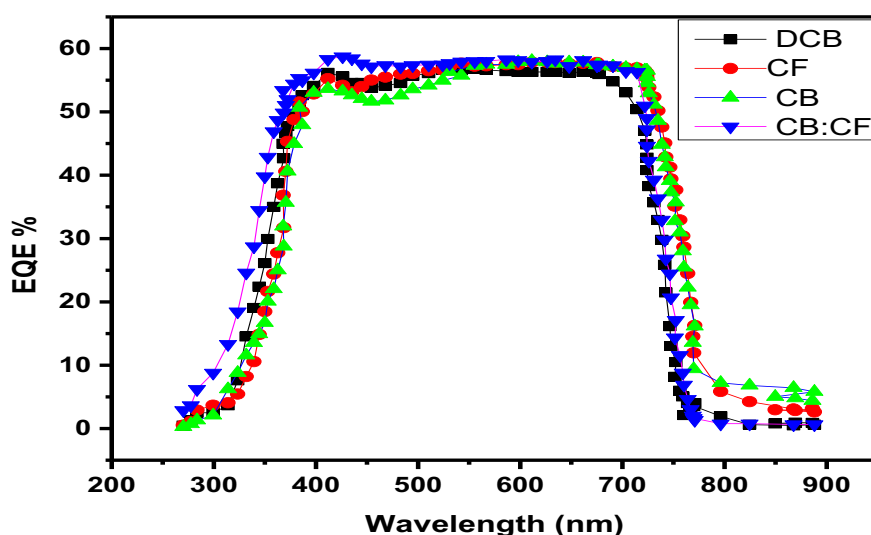


Figure 6: The EQE spectra of PEDO:PSS/P3HT: ZnONPs films in DCB, CF, CB, and CB:CF solvents.

The highest peak in external quantum efficiency can be attributed to P3HT:ZnONPs BHJ's crystalline structure and surface shape. The characteristic device parameters and current density versus voltage (J-V) curves for the short-circuit current density (J_{sc}), open-circuit voltage (V_{oc}), fill factor (FF), and power conversion efficiency (PCE) values of organic solar cells prepared with P3HT: ZnO NPs BHJ in several solvents are shown in Figure (6).

The current density (J) versus voltage (V) characteristics of the PEDOT:PSS/P3HT: ZnONPs devices are presented in Figure (7). The PV device parameters have been calculated using Eqs. (1) and (2) and are summarized in Table 2. The highest efficiency of 2.6% was obtained for the device which was subjected to (CB:CF) co-solvent while the lowest efficiency of 2.4% was associated with devices CB solvent devices. The increase in the device short circuit current can be explained by the increased roughness (R.M.S) of the polymer blend causing an increase in the contact area at the interface between the active layer and the Al cathode. This is thought to facilitate Al layer reshaping following the active layer surface morphology, and thus improving interfacial adhesion.

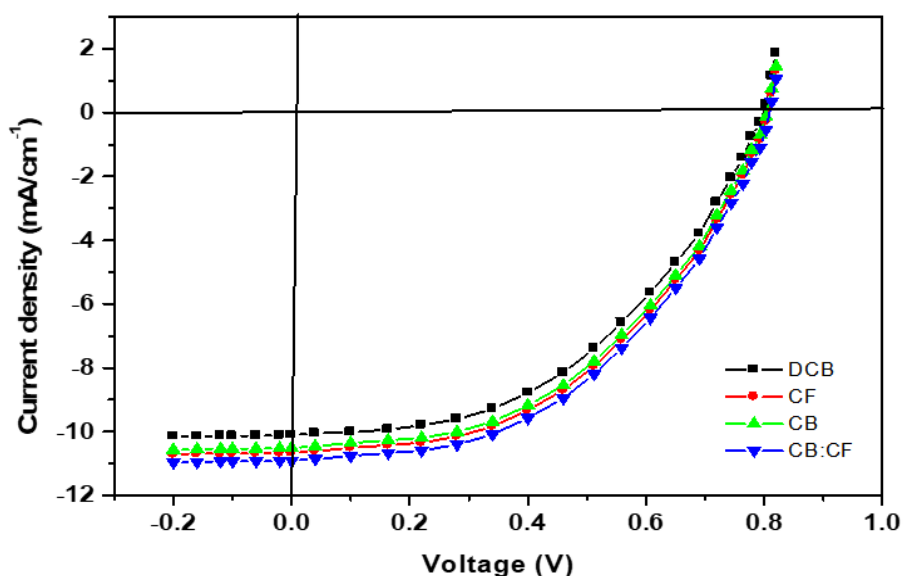


Figure 7: ITO/PEDOT: PSS /P3HT: ZnO nanoparticles /Al active layer ratio values of J–V curves for DCB, CF, CB, and CB:CF.

Table 2: The solar cell performance parameters of hybrid BHJ photovoltaic devices.

Device	V_{oc} (V)	FF	J_{sc} (mA/cm^2)	PCE (%)	R_s (Ω)	R_{sh} (Ω)
DCB	0.43	0.44	0.56	2.40	10.3	930
CF	0.46	0.49	0.74	2.46	12.4	965
CB	0.48	0.48	0.78	2.48	8.7	678
CB:CF	0.66	0.65	7.40	2.6	10.4	754

4. Conclusion

We built hybrid BHJ solar cell devices using a variety of solvents, including (CB), (DCB), (CF), and a co-solvent (CB: CF). Using UV-vis, XRD, PL, and Raman spectroscopy, the several solvents that affect the interchain interactions and crystallization of P3HT, ZnO NPs, and PEDOT: PSS buffer layer films was investigated. The device constructed from CB: CF co-solvent shows the enhanced performance of PCE by

2.6%. The mixed solvent's different solubility and evaporation rates affect the morphological structure, enhancing performance and increasing photocurrent and fill factor.

References

- [1] D. Chirvase, Z. Chiguvare, M. Knipper, J. Parisi, V. Dyakonov, and J. C. Hummelen, "Electrical and optical design and characterisation of regioregular poly(3-hexylthiophene-2,5diyl)/fullerene-based heterojunction polymer solar cells," *Synth. Met.*, vol. 138, no. 1–2, pp. 299–304, 2003, doi: 10.1016/S0379-6779(03)00027-4.
- [2] Terje A. Skotheim and John R. Reynolds, *CONJUGATED POLYMERS THEORY, SYNTHESIS, PROPERTIES, AND CHARACTERIZATION*, Third Edit. London: Taylor & Francis, 2007.
- [3] M. Reyes-Reyes, K. Kim, and D. L. Carroll, "High-efficiency photovoltaic devices based on annealed poly(3-hexylthiophene) and 1-(3-methoxycarbonyl)-propyl-1- phenyl-(6,6)C61 blends," *Appl. Phys. Lett.*, vol. 87, no. 8, p. 83506, Aug. 2005, doi: 10.1063/1.2006986.
- [4] T.-A. Chen, X. Wu, and R. D. Rieke, "Regiocontrolled Synthesis of Poly(3-alkylthiophenes) Mediated by Rieke Zinc: Their Characterization and Solid-State Properties," *J. Am. Chem. Soc.*, vol. 117, no. 1, pp. 233–244, Jan. 1995, doi: 10.1021/ja00106a027.
- [5] S. Cook, R. Katoh, and A. Furube, "Ultrafast Studies of Charge Generation in PCBM:P3HT Blend Films following Excitation of the Fullerene PCBM," *J. Phys. Chem. C*, vol. 113, no. 6, pp. 2547–2552, Feb. 2009, doi: 10.1021/jp8050774.
- [6] C. J. Keavney and M. B. Spitzer, "Indium phosphide solar cells made by ion implantation," *Appl. Phys. Lett.*, vol. 52, no. 17, pp. 1439–1440, Apr. 1988, doi: 10.1063/1.99095.
- [7] D. E. Carlson and C. R. Wronski, "Amorphous silicon solar cell," *Appl. Phys. Lett.*, vol. 28, no. 11, pp. 671–673, Jun. 1976, doi: 10.1063/1.88617.
- [8] Y. Ohtake, K. Kushiya, M. Ichikawa, A. Yamada, and M. K. Makoto Konagai, "Polycrystalline Cu(InGa)Se₂ Thin-Film Solar Cells with ZnSe Buffer Layers," *Jpn. J. Appl. Phys.*, vol. 34, no. 11R, p. 5949, 1995, doi: 10.1143/JJAP.34.5949.
- [9] V. Shrotriya, J. Ouyang, R. J. Tseng, G. Li, and Y. Yang, "Absorption spectra modification in poly(3-hexylthiophene):methanofullerene blend thin films," *Chem. Phys. Lett.*, vol. 411, no. 1–3, pp. 138–143, 2005, doi: 10.1016/j.cplett.2005.06.027.
- [10] O. Ourida and B. Said, "Influence of the blend concentration of P3HT: PCBM in the performances of BHJ solar cells," *SATRESET*, vol. 1, Jan. 2011.
- [11] U. Zhokhavets, T. Erb, H. Hoppe, G. Gobsch, and N. Serdar Sariciftci, "Effect of annealing of poly(3-hexylthiophene)/fullerene bulk heterojunction composites on structural and optical properties," *Thin Solid Films*, vol. 496, no. 2, pp. 679–682, 2006, doi: 10.1016/j.tsf.2005.09.093.
- [12] G. Li, V. Shrotriya, Y. Yao, J. Huang, and Y. Yang, "Manipulating regioregular poly(3-hexylthiophene) : [6,6]-phenyl-C61-butyric acid methyl ester blends—route towards high efficiency polymer solar cells," *J. Mater. Chem.*, vol. 17, no. 30, pp. 3126–3140, 2007, doi: 10.1039/B703075B.
- [13] H. Shen, P. Bienstman, and B. Maes, "Plasmonic absorption enhancement in organic solar cells with thin active layers," *J. Appl. Phys.*, vol. 106, no. 7, 2009, doi: 10.1063/1.3243163.
- [14] Dheyab, R.A., Hussein, A.A., Saeed, A.A., " Iraqi Journal of ScienceThis link is disabled. , vol. 62, no. 11, pp. 4342–4352, 2021, doi: [https://doi.org/10.24996/ijcs.2021.62.11\(SI\).15](https://doi.org/10.24996/ijcs.2021.62.11(SI).15)
- [15] B. Grévin, P. Rannou, R. Payerne, A. Pron, and J. P. Travers, "Multi-scale scanning tunneling microscopy imaging of self-organized regioregular poly(3-hexylthiophene) films," *J. Chem. Phys.*, vol. 118, no. 15, pp. 7097–7102, Apr. 2003, doi: 10.1063/1.1561435.
- [16] G. Li *et al.*, "High-efficiency solution processable polymer photovoltaic cells by self-organization of polymer blends," *Nat. Mater.*, vol. 4, pp. 864–868, Nov. 2005, doi: 10.1038/nmat1500.
- [17] M. Al-Ibrahim, O. Ambacher, S. Sensfuss, and G. Gobsch, "Effects of solvent and annealing on the improved performance of solar cells based on poly(3-hexylthiophene): Fullerene," *Appl. Phys. Lett.*, vol. 86, no. 20, p. 201120, May 2005, doi: 10.1063/1.1929875.
- [18] B. Kippelen and J.-L. Brédas, "Organic photovoltaics," *Energy Environ. Sci.*, vol. 2, no. 3, pp. 251–261, 2009, doi: 10.1039/B812502N.
- [19] M. Grätzel, "Photoelectrochemical cells," *Nature*, vol. 414, no. 6861, pp. 338–344, 2001, doi: 10.1038/35104607.